

CALCULATION OF RCCA WEAR REJECT CRITERIA IN NUCLEAR PLANTS

C. Bernaudat and K. Christodoulou

EDF/SEPTEN, 12-14 avenue Dutriévoz, F-69628 Villeurbanne, France

I. INTRODUCTION

1.1. Origin of the study : two similar incidents

1988, September 9th at DAMPIERRE 1 : during a refueling outage of the plant after the seventh operation cycle, a RCCA (Rod Control Cluster Assembly) shuffling was carried out. When the operators removed one of the RCCAs from the core, they saw that one of the absorber rodlets was broken. This rodlet fell into its corresponding guide-tube in the fuel assembly. The broken RCCA was examined by an eddy-current technique on the site, and then its upper part and the failed rodlet, which was extracted from the fuel assembly, were brought to EDF-GDL-SCMI for expertise.

1989, April 1st at GRAVELINES 4 : when setting the plant into cold stand-by, a RCCA remained blocked in an intermediate position (168 steps). After several maneuvering attempts, the RCCA was completely blocked between two positions : 152 and 168 steps from the bottom position. The upper internal containing the RCCA was removed and a televisual examination was made : once again, an absorber rodlet was missing ; it was cut near its upper end and fell into the fuel assembly. The removed upper internal was sent to EDF-GDL-SCMI for full examination.

1.2. Examination results

Visual examination of the broken rodlets showed that, in both cases, the rupture occurred at the level of a through-wall scar which was due to fretting between the rodlet cladding and the seventh guide-card. The localization of the scar corresponded to the 7th guide-card when the RCCA was in its normal parking position (225 steps) during operation. The scars looked like roughly rectangular windows, with round corners and sharp-edged sides. The rupture is localized near the upper end of the scar, just at the junction between the vertical sides and the round corners of the wear windows, and just 1 to 2 millimeters over the upper end of the absorber Silver-Indium-Cadmium (SIC) internal rodlet. A visual examination of the lower parts of the broken rodlets and of the other rodlets revealed large through-wall scars corresponding to the level of the 4th, 5th and 6th guide-cards.

The broken rodlets were cut and the 6th and 7th guide-card wears have been measured : the measurements confirmed that some of the 6th guide-card scars were more severe than the ones which caused rodlet ruptures, although no cladding crack or failure was observed there ; some wear values (percentages of missing cladding cross-sections) are gathered in table 1. The cross-section of a worn cladding area is shown on figure 2. The most affected RCCAs were those which mainly remain at the same position, which induces concentrated wear on the rodlet cladding, just at the level of the guide-cards (shut-down RCCAs).

Table 1 : Characteristics of DAMPIERRE 1 and GRAVELINES 4 broken RCCAs

Plant	DAMPIERRE 1	GRAVELINES 4
RCCA no. and core location	24A004E (B6)	24A00N1(K8)
Location of broken rodlet in assembly	C12	F15
% of wear at 7th card level	29%	38%
% of wear at 6th card level	42%	N.A.

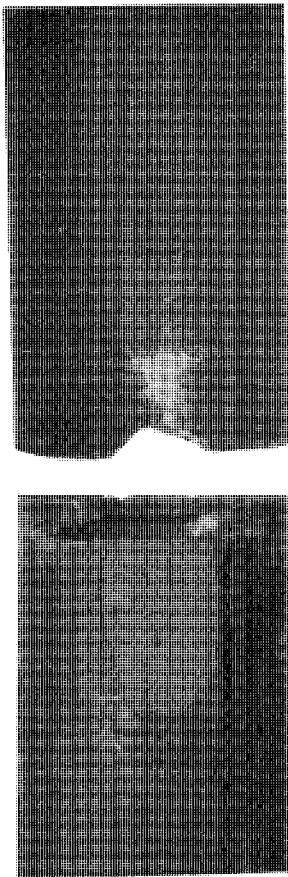


Figure 1 : Aspect of the ruptured area of DAMPIERRE rodlet

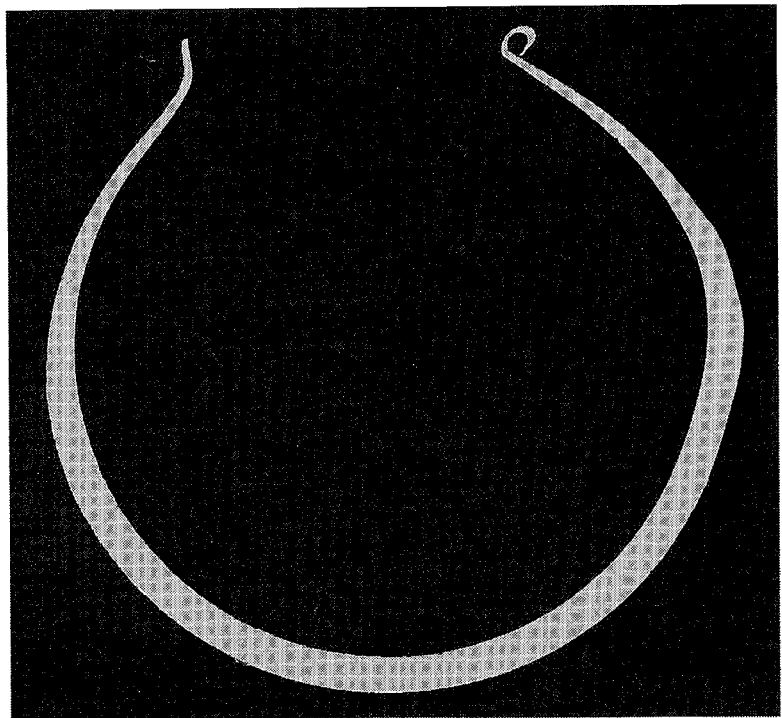


Figure 2 : Cross section of 7th-card worn area of DAMPIERRE rodlet

The rupture facieses have been examined by SEM techniques : both ruptured rodlets showed regular stripes, which clearly indicate that the failures were caused by fatigue damage. Two cracks initiated at the same time, starting from the upper corners of the wear windows, as described before. The cracks propagated by fatigue due to cycling stresses induced by step-by-step movements of the RCCAs and hydraulical vibrations. When each crack rejoined the other one, at the opposite side from the wear window, a final ductile rupture occurred, with a strong striction. Figure 3 is a SEM photograph of the rupture facies observed on the DAMPIERRE failed rodlet, where fatigue stripes are clearly visible.

The expertises of both rodlets showed that the 7th card-level wear was particularly important in the rupture process, and that it was a generic problem which could affect all the French 900 MW power plants, i.e. 34 reactors. Thus, studies have been made in France, both by EDF and FRAMATOME, in order to understand the whole problem and prevent this kind of incident in the future.

The present paper describes the work performed by EDF since 1989. It can be divided into three different tasks, each of them being interrelated with the others :

- mechanical analysis of the worn rodlet cladding ; this task includes both a static and dynamic analysis to determine the external loadings on the cladding and the resulting stresses in the worn area ;
- determination of the wear kinetics, in order to calculate the fatigue damage in a rodlet with a time-increasing wear, and then its in-reactor lifetime ;
- elaboration of a more accurate RCCA management strategy.

The result of these complementary tasks is a set of RCCA removal criteria tables, which has now been successfully included in all the 900 MW plant operation specifications, for more than two years.

II. MECHANICAL ANALYSIS OF A WORN RODLET

II.1. Worn area meshing

The first part of this study was to build a mesh of a rodlet cladding including an area worn by fretting against a guid-card. In a previous study made in 1987, a shell-element mesh was built, but this approach didn't allow modelling cladding thickness reduction in the neighbourhood of the wear window, or non-through-wall scars. So we chose cubic massive elements to achieve the mesh, which had to reproduce, as exactly as possible, the shape of the scar, and especially the sharp-edged sides of the wear window. Particular care was taken to model properly the junction between the horizontal and vertical sides of the window. Both non-through-wall and through-wall scars were modeled, in order to cover the whole evolution of the wear with time. Figure 4 shows the massive-element mesh of a rodlet cladding, in the neighbourhood of a through-wall scar.

For the whole study, only a cladding portion whose length was equal to the distance between two consecutive guide-cards was considered. A short part of this cladding was meshed with massive elements, as described above, and the remaining part of the structure was modeled by an equivalent beam. A short and rigid annulus ensured the junction between massive and beam elements of the structure.

The computer code used for both mesh building and stress-strain calculations is CASTEM 2000 [1], which has been developed by CEA. It was run on a CRAY-YMP computer.

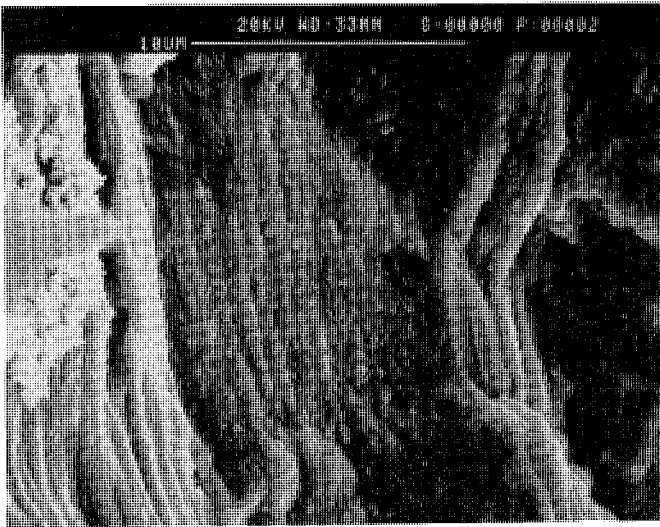


Figure 3 : SEM photograph of crack facies in DAMPIERRE broken rodlet

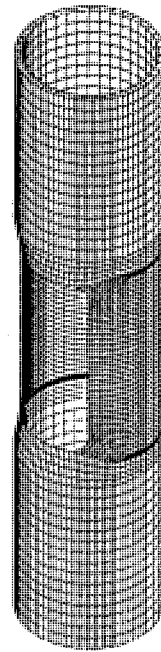


Figure 4 : 3D-massive element mesh of a worn area with a through-wall scar

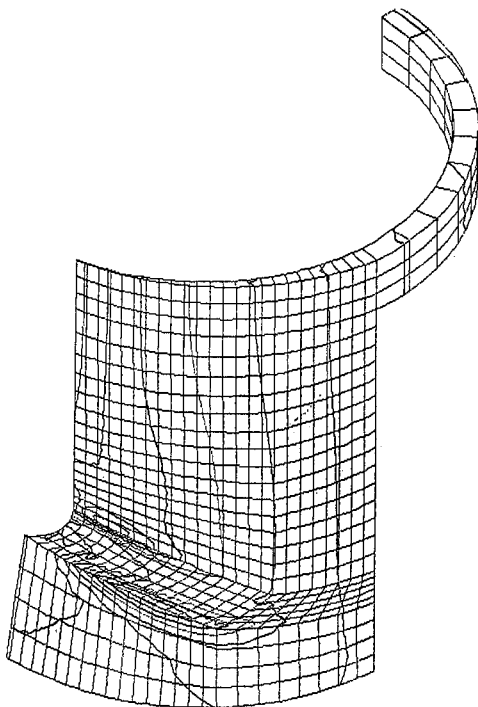


Figure 5 : result of stress calculation in the neighbourhood of a through-wall scar

II.2. External loadings

The two major sources of external mechanical loadings which had to be applied on the structure described above are : an axial force due to step-by-step vertical movements of the RCCA and lateral vibrations due to hydraulical turbulences.

Step-by-step movements, caused by the RCCA maneuvering device, induce an axial force in the rodlet cladding. This force is alternatively tensile and compressive and its extreme values have been determined in full-scale experiments.

Hydraulical vibrations cause essentially lateral displacements, which are limited by the gap between the rodlets and the holes machined in the guide-cards.

It is easy to understand that the tensile-compressive axial force induce both tensile-compressive and bending stresses in the worn area of the cladding, because the cross-section of this worn area is eccentered from the rodlet axis. Moreover, the hydraulical vibrations cause additional bending stresses and strains. The vibration-induced stresses vary very rapidly, but even with large through-wall scars (i.e. more than 40% of the cross-section), these stresses remain below the endurance limit of the cladding material (AISI 304 austenitic steel). So it is possible to cumulate all the external loads (axial tensile force with a bending moment which "opens" the wear window, and compressive force with a bending moment which "closes" it) in order to calculate the maximum stress amplitude, and then, the number of stress cycles (i.e. step-by-step movements) leading to cladding failure by fatigue.

II.3. Mesh verification

In order to check the mesh described above, two verifications have been made : a qualitative one to verify if the maximal stresses were localized in the area where the fatigue cracks initiated, and a quantitative one, by comparison between the stresses obtained with both the shell-element mesh and the massive-element mesh. This second verification was made with two major differences between the meshes : the shape of the structure (thickness reduction near the edge of the window, with massive elements) and the mesh size in the location of the fatigue cracks, which was smaller with shell-elements. The number of degrees-of-freedom was approximately 35,000 in the massive-element mesh, i.e. twice the one of the shell-element mesh.

Figure 5 (previous page) shows the result of stress calculations in the neighbourhood of the scars. As can be seen, the maximal stresses are concentrated in a very small area which lies just near the edge of the wear window, and at the junction between its vertical side and round corner.

The second verification was carried out as follows : with both meshes, submitted to the same external loadings, the stresses were calculated. By varying the wear percentage, the maximal wears leading to equivalent Tresca stresses which met the ASME [2] requirements were determined. Table 2 shows the wear percentages obtained with both meshes, corresponding to stresses obeying the indicated ASME requirements. It can be noted that in both cases, the wear criteria are very similar, and even a little bit less severe with the massive-element mesh than with the shell-element one. This is due to the fact that with the same wear percentage, the worn cross-section is less eccentered with the massive-element mesh, and so, the bending moment due to the axial force is lower.

II.4. Calculations of fatigue damage factors

In the next step we had to calculate the fatigue damage factors, i.e. the fatigue damage induced by one stress cycle in the structure. These factors were calculated with non-through-wall and through-wall worn claddings, at every 6° around the cladding circumference, starting from the edge of the wear window. The factors calculated with through-wall scared cladding have been established with wear windows subtending angles growing by steps of 6° . So it is possible to

accumulate fatigue damage in the same location of the cladding, while the wear is increasing by fretting. Figure 6 shows how the fatigue damage factors were calculated.

Table 2 : Wear criteria meeting ASME requirements with massive and shell-element meshes

Type of mesh	shell elements	massive elements
Primary membrane plus flexion stress	36.5%	37.3%
Primary + secondary stress amplitude	40%	43%
Peak stress (fatigue analysis) : axial force + vibrations	16% to 36%(*)	19.5 to 35.8%(*)
Peak stress (fatigue analysis) : axial force	28% to 40%(*)	31% to 41.8%(*)

(*) depending on the RCCA groups, which have different numbers of step-by-step movements per cycle.

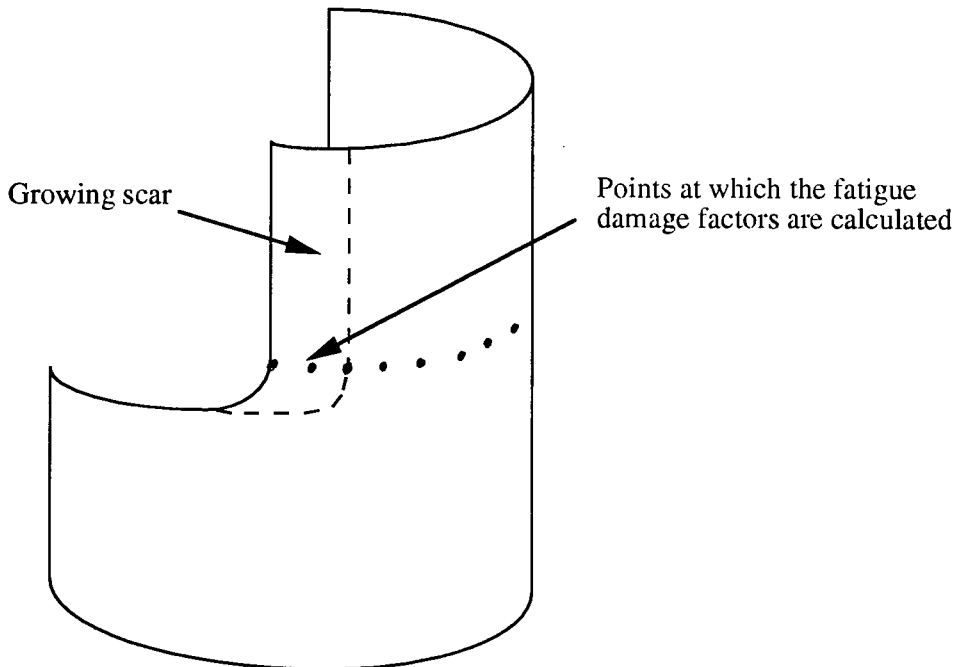


Figure 6 : calculation method for cumulative fatigue damage factors.

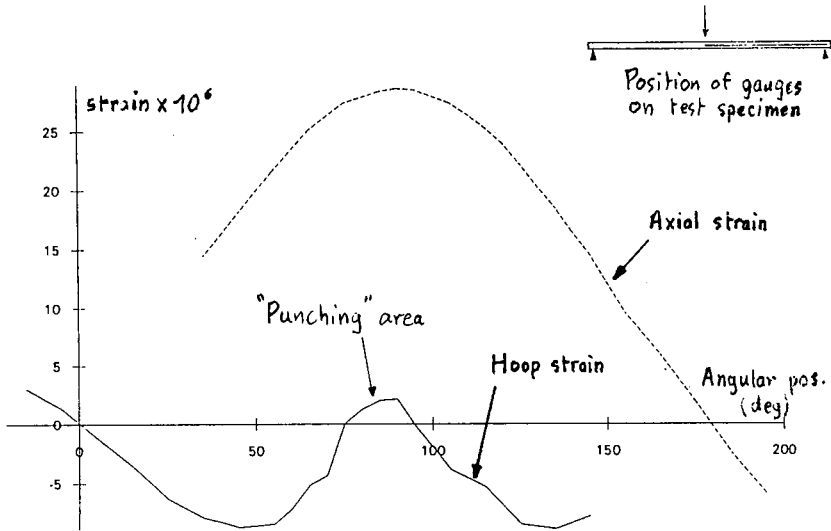


Figure 7 : Result of bending test showing clad "punching" by SIC rodlet

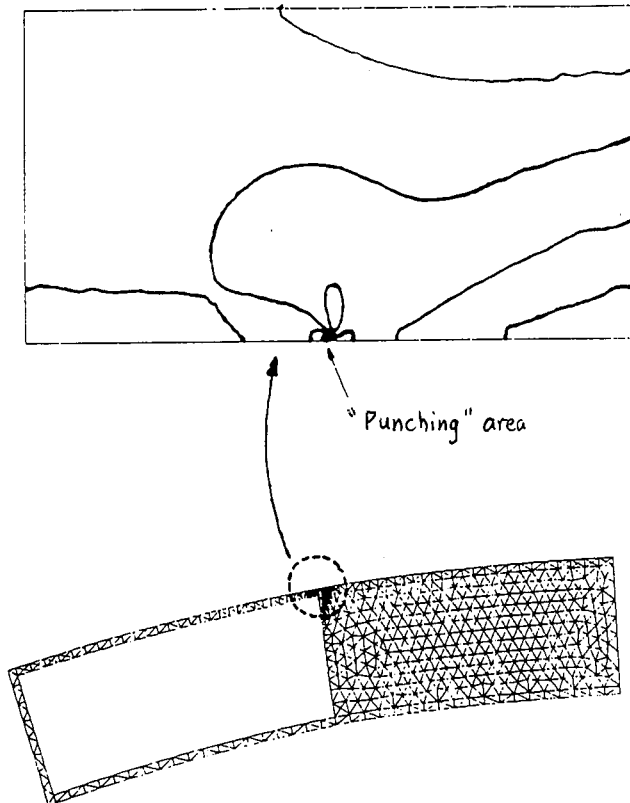


Figure 8 : 2D-finite-element calculation showing stress concentration in the "punching" area

II.5. The particular case of the 7th-card-level wears

As was mentioned in the introduction, the rodlets didn't fail in the location of the largest scars. This is not so surprising when we see that the 7th-card-level wear corresponds to the upper end of the SIC rodlet. Moreover, the 7th guide-card is a supporting point of the rod, when excited by flow-induced lateral vibrations. This causes local mechanical effects which have to be determined. To do this, bending tests and dynamical analyses have been made.

II.5.1. Bending tests

Bending tests were carried out on specimens which reproduced the upper part of an absorber rodlet, with its internal SIC rodlet and hold spring (whose compressive strength could be adjusted with a screw). In these tests, the influence of spring force and SIC rodlet upper end shape (chamfered or not) were examined. The result is that, with both chamfered and standard SIC rodlet shapes, bending induces a local "punching" in the cladding. This effect appears when axial and hoop strain are measured simultaneously with strain gauges.

In an empty cladding, or far from the end of the SIC rodlet, when the bending force causes an axial tensile stress in the generatrice where the 2D-strain gauge is stuck, the axial strain is positive and, due to Poisson's ratio, the hoop strain is negative.

But when the gauge is localized just at the level of the upper part of the internal SIC rodlet, the hoop strain becomes positive. This effect, where both axial and hoop strains are positive, has thus been called "punching". It is very localized and so, it couldn't be determined quantitatively with strain gauges. Figure 7 shows the results of the strain measurements obtained during these tests : the "punching" of the cladding is clearly visible.

To assess this effect quantitatively, a 2D-finite-element calculation was made, as shown on figure 8. Even with a very refined mesh in the "punching" area, the stress concentration factor is approximately 1.5. In order to take into account this stress concentration due to clad punching, this factor was applied to the total bending stress just on the edge of the wear window, because when the rodlet is bent, the upper end of the SIC rod "punches" the cladding here.

II.5.2. Dynamic analyses

The bending moments due to hydraulical vibrations were determined, both at the level of the 7th guide-card and the others. This was done by the means of a dynamic analysis of the whole RCCA, considering the eigenmodes of vibration (up to a frequency of 20 Hz) and all the geometrical limitations of these vibrations. The values obtained by the means of this dynamic analysis were 0.3 Nm in the current wear area (1st to 6th guide-cards) and 0.8 Nm at the level of the 7th guide-card. This higher value increases the stresses in the 7th-card-level wears and reinforces the nocivity of such wears.

II.5.3. Mechanical particularities of 7th-card wears

The 7th-card-level wears present thus two particularities : local "punching" of the cladding by the upper end of the SIC rodlet and larger bending moments due to hydraulical vibrations. These two effects are cumulative ; they contribute to increase the stresses in the worn areas and cause rupture by fatigue crack propagation, although the 7th-card-level scars are not always the largest ones.

III. WEAR KINETICS

In parallel with the mechanical analysis of a worn rodlet, wear kinetics has been studied and an empirical model has been established. The available data for the wear kinetics modelization were wear measurements coming from CRUAS 2, at EOC 2, 3 and 4. Circa 200 wears were successively measured after 2, 3 and 4 operating cycles, so that the wear evolution could be evaluated. The model is built as follows.

If we suppose that the wear kinetics obeys a power law versus time, we get :

$$U(t) = A.t^B \quad (1)$$

where t is the time (in number of cycles), U is the wear percentage at time t and A , B are empirical coefficients.

When applying this model to each triplet of wear measurements, two correlations appear :

- between $U(2)$ and A (which is the estimated wear after 1 cycle) :

$$A = -0.035 + 0.744U(2) \quad (2)$$

- between A and B :

$$B = 2.889.exp(-0.657(A^{0.5})) \quad (3)$$

So, for any wear measurement $U(n)$ obtained after a given number of cycles n , it is possible to determine a wear kinetics law with the following algorithm :

- a) estimation of a first guess for the wear at EOC 2 :

$$U(2) = U(n).(2/n) \quad (4)$$

- b) calculations of A and B using eqns (2) and (3) ;

- c) estimation of a new guess for $U(2)$:

$$U(2) = U(n).(2/n)^B \quad (5)$$

- d) iteration on steps b) and c) hereabove, until convergence is reached.

In order to check the model, the wears of all the CRUAS 2 measured rodlets have been estimated by the model and compared to the experimental values. The model leads to a correct and quite conservative wear prediction, both for EOC 3 and EOC 4, as shown on figure 9.

IV. RCCA MANAGEMENT STRATEGY

A new RCCA management strategy has been established by EDF's Nuclear Plant Exploitation Division (EPN). This strategy aims to increase the RCCA in-reactor lifetime and is described below.

The RCCAs are divided into five groups, each of them being characterized by a specific number of step-by-step movements per cycle. No shuffling of RCCAs in a group or between different groups is allowed. At each end of cycle, the parking position of the RCCAs is modified. Three parking positions are used during three successive operating cycles : 222, 225 and 228 steps. The 3-step difference between two neighbouring positions has been introduced to avoid wear superposition, because the uncertainty in the position is +/- one step. All the RCCAs are controlled and wears are measured (by both ultrasonic and eddy-current techniques) after every 3 cycles, that is, after the RCCAs stood in the core during one cycle in each of the three parking positions.

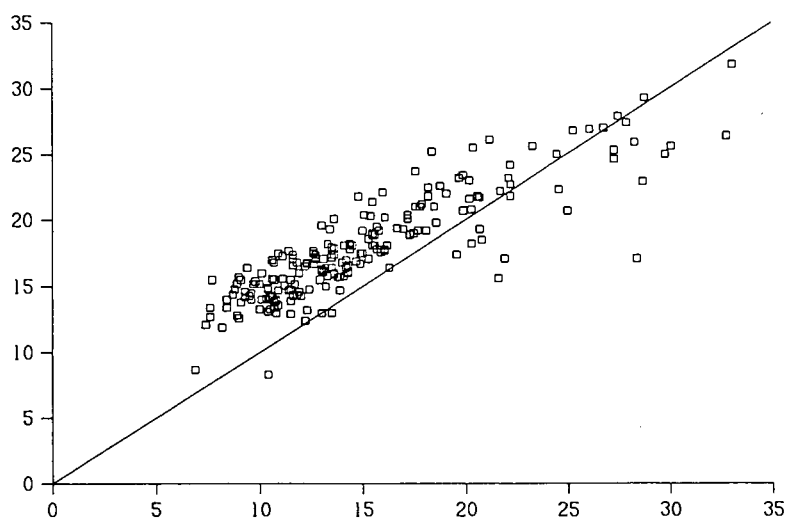
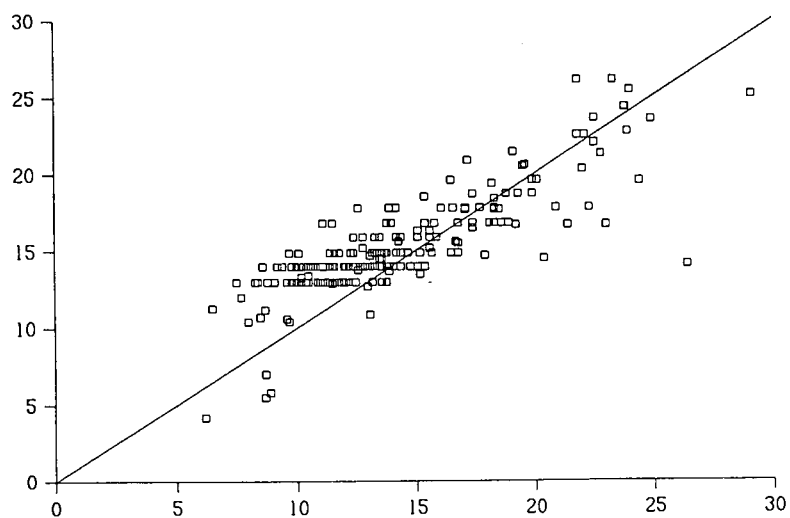


Figure 9 : Wear kinetics : comparison of predicted vs. measured wears :
- top : prediction of EOC3 wear knowing EOC2 wear ;
- bottom : prediction of EOC4 wear knowing EOC3 wear.

So, based on wear reject criteria tables (whose determination is described in the next chapter), the operator can take his decision after having controlled a RCCA :

- immediate removal ;
- delayed removal (after 1 or 2 extra cycles, without any intermediate control) ;
- waiting 3 extra cycles to take a new decision after the next control.

V. WEAR REJECT CRITERIA TABLES

First, it is easy to understand that the wear reject criteria will depend :

- on the RCCA group, characterized by its specific number of step-by-step movements per cycle (from 15,000 for a shut-down group up to 500,000 for a regulation group, during load-following operation) ;
- on the wear location, with special criteria to be applied to 7th-card-level wears ;
- on the RCCA management strategy. With the one presented hereabove, a wear increases during only one cycle between two successive controls. The calculation of cumulative fatigue damage must take this wear evolution versus time into account.

For a given wear percentage obtained during RCCA control no. n (i.e. after $3n$ cycles in reactor and n "wearing" cycles for each parking position), the wear kinetics law is estimated (cf. chap. III above). Then the cumulative fatigue damage is calculated, taking into account the fact that during three cycles, the wear increased during the first one and remained at its final value during the last two (this point doesn't apply to the regulation groups, whose wears are spread and increase during all the cycles) and the number of step-by-step movements, which is namely the number of stress cycles in the worn areas of the rodlet cladding. When the cumulative damage reaches 1 during a given cycle, a fatigue crack may initiate and propagate, causing rapidly rodlet rupture. So the RCCA must be removed from the core at the end of the previous cycle.

So, for a given control (let's say no. n), a large domain of wears percentages is explored, and for each one, wear kinetics, fatigue damage and RCCA lifetime are evaluated. The reject criteria for immediate removal (lifetime = $3n$ cycles), delayed removal (lifetime = $3n+1$ or $3n+2$ cycles) or waiting the next control (lifetime = $3n+3$ or more) can then be calculated in all the cases. An example of wear reject criteria table is presented in table 4. This has been done for controls no. 1 to 4, i.e. for RCCA lifetimes up to 14 cycles.

Table 4 : example of wear reject criteria table.

Control no.	1	2	3	4
Immediate removal	28.3-29.9%	25.9-26.9%	25.0-25.5%	24.6-24.9%
removal after 1 extra cycle	26.9-28.3%	25.1-25.9%	24.6-25.0%	24.3-24.6%
removal after 2 extra cycles	25.6-26.9%	24.5-25.1%	24.2-24.6%	24.0-24.3%
waiting for the next control	< 25.6%	< 24.5%	< 24.2%	24.0%

VI. CONCLUSION

The new RCCA management strategy, coupled with the wear reject criteria tables, has been applied to all the 900 MW French power plants (34 reactors). A transition phase, with special criteria, has been carried out during the first two years (1990 and 1991), as long as "old" RCCAs remained in the cores. The new strategy reached its "full power" in 1992 and allows now both safety and economical improvements : application of a unique strategy with a unique set of reject criteria, taking into account all the mechanical effects and the evolution of the cladding wears, allows preventing rodlet rupture in the future and the increase plant operation safety ; moreover, this has been done with an increased RCCA expected lifetime, which leads to large economical benefits.

Such a large study has been supported by a lot of participants :

- EDF (many departments) : whole study supervision, static and dynamic analyses of worn RCCAs, wear kinetics modelization, elaboration of RCCA new management strategy, expertises of broken rodlets, wear measurements and wear database constitution, full-scale vibration experiments, theoretical aspects of mechanical effects on 7th-card-level wears ;
- FRAMATOME : full-scale experiments to determine the external loadings applied on the RCCAs, financial and technical participation to the expertises of broken rodlets and bending test specimen design and supplying ;
- INSA Lyon : performing rodlet bending experiments.

REFERENCES

- [1] P. VERPEAUX, A. MILLARD, T. CHARRAS and A. COMBESURE :
"A Modern Approach of Large Computer Codes for Structural Analysis"
SMiRT 10, August 1989, Vol. B, p. 75.
- [2] ASME Boiler and Pressure Vessel Code :
Section III, Division 1 - Subsection NG